PHASE DOPPLER INTERFEROMETRY MEASUREMENTS IN WATER SPRAYS PRODUCED BY RESIDENTIAL FIRE SPRINKLERS

by

John F. Widmann
Building and Fire Research Laboratory
National Institute of Standards and Technology
Gaithersburg, MD 20899, USA

Reprinted from Fire Safety Journal, Vol. 36, No. 6, 545-567, September 2001

NIST
National Institute of Standards and Technology
Technology Administration, U.S. Department of Commerce

ELSEVIER

Fire Safety Journal 36 (2001) 545–567

FIRE SAFETY JOURNAL

www.elsevier.com/locate/firesaf

Phase Doppler interferometry measurements in water sprays produced by residential fire sprinklers

John F. Widmann*

Building and Fire Research Laboratory, National Institute of Standards and Technology, 100 Bureau Drive, Stop 8653, Gaithersburg, Maryland 20899-8653, USA

Received 6 November 2000; received in revised form 23 January 2001; accepted 1 February 2001

Abstract

A phase Doppler interferometry (PDI) system was used to characterize the water sprays produced by four residential fire sprinklers. Four pendent sprinklers with K-factors ranging from $7.2 \times 10^{-5}\,\mathrm{m^3\,s^{-1}\,kPa^{-0.5}}$ ($3.0\,\mathrm{gal\,min^{-1}\,psig^{-0.5}}$) to $1.35 \times 10^{-4}\,\mathrm{m^3\,s^{-1}\,kPa^{-0.5}}$ ($5.6\,\mathrm{gal\,min^{-1}\,psig^{-0.5}}$) were investigated. The measurements include characteristic size (arithmetic mean diameter, volume mean diameter, Sauter mean diameter), mean velocity (axial and radial components), and liquid volume flux. The effect of water pressure on drop size was also investigated. The mean drop size (flux-averaged volume diameter, $\overline{D_{30}}$) was found to be proportional to $P^{-1/3}$ over the range $93\,\mathrm{kPa} \leqslant P \leqslant 200\,\mathrm{kPa}$. Published by Elsevier Science Ltd.

Keywords: Fire sprinklers; Water sprays; Drop size measurement; Phase Doppler interferometry; Drop velocity measurement

1. Introduction

1.1. Sprinkler characterization

The fire sprinkler is the most commonly used fire protection system, and it has been reported that the average fire loss in properties protected by sprinklers is about 10% of that in non-protected properties [1]. The basic function of a fire sprinkler is

*Corresponding author. Tel.: +1-301-975-2488; fax: +1-301-975-4052.
E-mail address: john.widmann@nist.gov (J.F. Widmann).

0379-7112/01/$ - see front matter Published by Elsevier Science Ltd.
PII: S0379-7112(01)00009-1

Nomenclature

d_i	diameter of the ith size class
D_{10}	arithmetic mean diameter
D_{30}	volume mean diameter
$\overline{D_{30}}$	flux-averaged mean volume diameter
D_{32}	Sauter mean diameter
F_v	volume flux
k	coverage factor
K	sprinkler K-factor
n_i	counts in the ith size class
P	pressure
r	radial coordinate
R	correlation coefficient
s	standard deviation of replicated samples
U_c	combined standard uncertainty
v_z	axial velocity
v_r	radial velocity
V	volumetric flow rate

Greek letters

λ	wavelength, nm
θ	angular coordinate

to extinguish or control an accidental fire. The effectiveness of the sprinkler spray at controlling a fire is governed by the spray characteristics (e.g., spatial distributions of drop size, drop velocity, mass flux). For example, large drops can penetrate a rising fire plume to reach the fire source and wet combustible materials adjacent to the fire, whereas smaller drops will be entrained in the buoyant plume and carried away from the fire. Furthermore, the evaporating smaller drops have a cooling effect on the hot gases, and in some cases have been observed to prevent additional fire sprinklers from activating. It is therefore important that the spray characteristics of fire sprinklers be understood if the interaction of the spray and the fire is to be understood and predicted. The reader is referred to the recent review by Grant et al. [2] for a thorough discussion of fire suppression by water sprays.

The rapid increase in computer technology has permitted increasingly more sophisticated modeling of the dynamics of fires. In particular, it is now possible to include the effect of water sprays on the fire dynamics, and to account for the complex interaction of this multiphase combustion process. For example, the fire dynamics simulator (FDS) developed at the National Institute of Standards and Technology (NIST) is being used to predict large-scale fire phenomena [3,4] in a variety of fire scenarios. However, to include the effect of fire sprinklers on the fire dynamics it is necessary to provide characteristics of the water spray produced by

the sprinklers. This information cannot be accurately predicted and must be experimentally determined.

Previous studies characterizing fire sprinkler sprays have utilized photographic techniques [5–8] and a laser-light shadowing method [9–12]. The photographic methods included illuminating the drops using strobe lighting and pulsed lasers, and using still photographs and video cameras for image capture. The laser-light shadowing technique utilized a modified commercially available instrument intended for cloud drop measurements. The drops were sized by determining the number of pixels shadowed as the drops passed through a visible laser-light sheet illuminating a linear photodiode array. One component of the drop velocity was also determined by the length of time the pixels were shadowed.

More recently, Sheppard et al. [13] demonstrated that particle image velocimetry (PIV) can be used to measure droplet velocities in the sprays produced by residential fire sprinklers. Unfortunately, the PIV technique does not provide information on the droplet size distributions or size–velocity correlations. At the same conference, Gandhi and Steppan [14] presented phase Doppler interferometry (PDI) measurements in industrial fire sprinkler sprays. They compared their volume flux measurements with pan test measurements, in which the spray was collected in pans for a known period of time, resulting in an independent volume flux measurement. They reported that the comparison was poor when the guage pressure at the sprinkler head was 48.3 kPa (7 psig), but considerably better when the guage pressure at the sprinkler was 153.1 kPa (22.2 psig). The correlation coefficients were 0.5259 and 0.8912 for the former and latter cases, respectively. Presumably, the increase in pressure resulted in significant changes in the spray characteristics, likely shifting the size distributions towards the smaller drops. They also reported a correlation coefficient of 0.9993 when PDI volume flux measurements were compared with pan test measurements for a water mist nozzle. Size and velocity distributions were not presented; however, a figure showing the variation of drop diameter with time suggests that the data correspond to a bimodal size distribution. The authors did not report the uncertainty in the measurements, but the good agreement between the PDI volume flux measurements and the pan test measurements (for the sprinkler at 153.1 kPa and the water mist nozzle) suggested that PDI may be a promising technique for characterizing fire sprinkler sprays.

Following the initial work of Gandhi and Steppan, Widmann [15] reported the results of a feasibility study to asses the accuracy of PDI measurements in water sprays produced by residential fire sprinklers. A single fire sprinkler was characterized, and the uncertainty in the measurements quantified. The results of that study indicate that accurate size and velocity measurements can be obtained in residential fire sprinkler sprays using PDI. For example, the uncertainties[1] in the arithmetic mean diameter and volume mean diameter were reported to be 6.4% and 4.1%, respectively. Mean velocity measurements were reported with uncertainties of 6.9% (axial velocity) and 8.4% (radial velocity). This paper is a follow-up to that

[1] Unless otherwise stated, all uncertainties reported herein correspond to the combined standard uncertainty, U_c, with a coverage factor, $k = 2$ (i.e., $2U_c$) [16,17].

initial feasibility study, and presents the results of a study in which PDI was used to experimentally characterize four residential fire sprinklers. The effect of water pressure on the drop size was also investigated.

1.2. Phase Doppler interferometry (PDI)

Since its introduction, phase Doppler interferometry has been used to characterize sprays in a wide variety of areas including spray combustion, spray coatings, agricultural pesticides, fire suppression, and others. PDI, which is an extension of laser Doppler velocimetry that measures droplet size as well as velocity [18–20], involves creating an interference pattern in the region where two laser beams intersect, resulting in a region of alternating light and dark fringes. The region where the laser beams intersect is called the *probe volume* or *sample volume*. Due to the interference pattern, a droplet passing through the probe volume scatters light exhibiting an angular and temporal intensity distribution which is characteristic of the size, refractive index, and velocity of the droplet. For a droplet with known refractive index, the size and velocity can be determined by analyzing the scattered light collected with several photomultiplier tubes (PMT). Additional details on the phase Doppler method are available in Ref. [21].

2. Experimental

A sprinkler characterization facility was constructed in the Building and Fire Research Laboratory at NIST for the purpose of characterizing fire sprinklers and water mist suppression systems. The facility, presented in Fig. 1, consists of an enclosed area equipped with the necessary piping and pumps to operate under a variety of flow conditions. The water is collected and recirculated back to the sprinkler, forming a closed-loop system. The total dimensions of the enclosed pool used to collect the water spray is $6\,m \times 6\,m$, and the sprinkler can be mounted at one of several ports 1.6 m above the floor. A variety of diagnostics are being investigated for use in the facility to characterize the water sprays produced by fire sprinklers and mist generation systems.

The measurements presented here were obtained in the sprays generated by four residential fire sprinklers. The sprinklers studied are listed in Table 1 and shown in Fig. 2. The sprinklers that were characterized are common fire sprinklers for residential applications, and were operated under typical conditions. The sprays produced by fire sprinklers are large compared to systems in which PDI is typically applied, and cover an area on the order of $10\,m^2$. Due to the large coverage area, it is necessary to locate the PDI transmitting and receiving optics directly in the spray. This was accomplished by encasing both the transmitting and receiving optical systems in water-tight containers equipped with a purge of dry air to prevent moisture from condensing on the optics. The PDI optics are mounted to a rectangular translation stage that can be moved in either horizontal direction. The

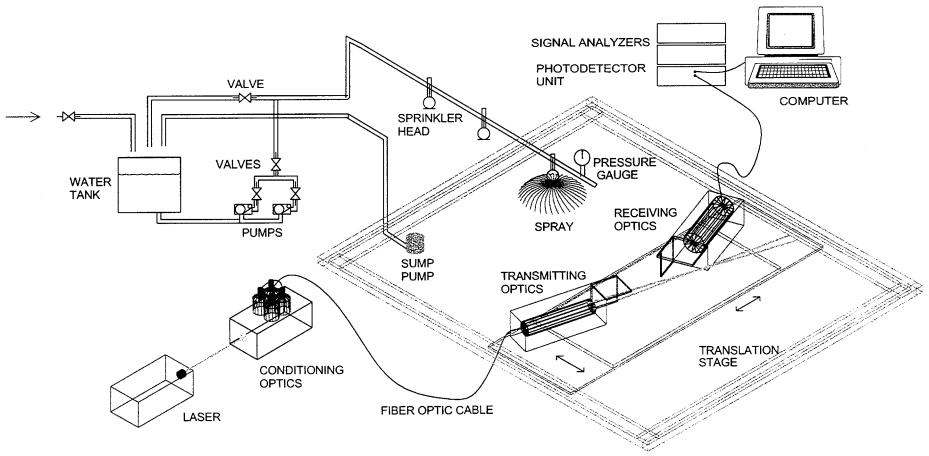

Fig. 1. Schematic of the experimental facility.

Table 1
The K-factors reported by the manufacturers and the operating pressures for the residential fire sprinklers used in this study

Sprinkler	K-factor ($m^3\,s^{-1}\,kPa^{-0.5}$)	Operating pressure (kPa)
A	0.72×10^{-4}	103 ± 7
B	0.75×10^{-4}	172 ± 7
C	1.35×10^{-4}	131 ± 7
D	1.35×10^{-4}	131 ± 7

measurements were obtained in a horizontal plane 1.12 ± 0.01 m below the sprinkler deflector plate.

The experiments were conducted using a 2-component phase Doppler interferometer with a real-time signal analyzer (RSA) available from TSI, Inc.[2] A 300 mW air-cooled argon ion laser operating in multi-line mode was used as the illumination source, and the green ($\lambda = 514.5$ nm) and blue ($\lambda = 488$ nm) lines were used to measure the axial and radial velocity components, respectively. The laser beams are split and focused by the beam conditioning optics and the transmitting optics, respectively. The laser beams intersect at the sample volume, where they create a fringe pattern. As a drop passes through the sample volume (see Fig. 3A) the scattered light is collected by the receiving optics, and the size and velocity of the drop are determined.

The transmitting optics were coupled to the beam conditioning optics using fiber optic cables, which permitted the transmitting optics to be located in the spray. The

[2] Certain commercial equipment, materials, or software are identified in this manuscript to specify adequately the experimental procedure. Such identification does not imply recommendation or endorsement by the National Institute of Standards and Technology, nor does it imply that the materials or equipment are necessarily the best available for this purpose.

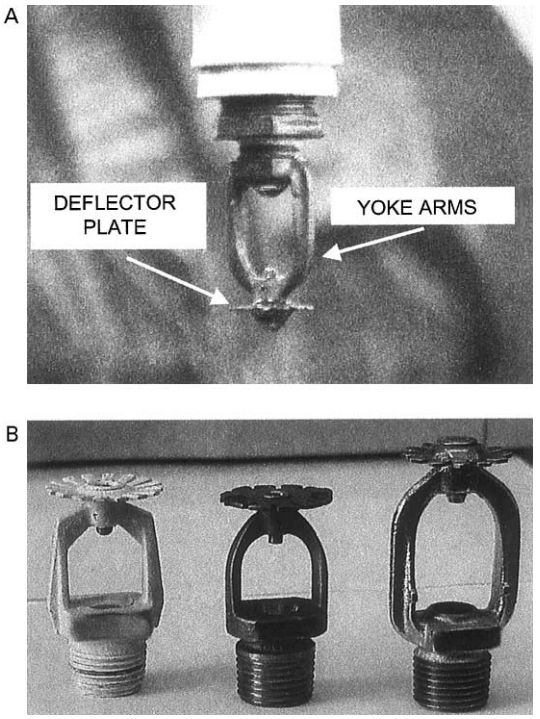

Fig. 2. Photographs of (A) one of the residential sprinklers showing the yoke arms and deflector plate, and (B) the other sprinklers characterized in this study.

front lens on the transmitting optics had a focal length of 1000 mm, and a 50 mm extender was used to increase the maximum measurable drop size to 950 μm. The receiving optics were located at a scattering angle of $33^\circ \pm 1^\circ$ measured from the direction of propagation of the laser beams. The relatively long focal lengths of the front lenses on the receiving and transmitting optics necessitate a relatively large translation stage, and limit how close the probe volume can be located to the walls of the enclosed area.

The PDI signal processor was initially operated with the sampling settings recommended by the manufacturer for the flow investigated (mixer frequency = 36 MHz, sample frequency = 40 MHz, low pass filter = 20 MHz), although it was found that the system operated more effectively under other settings. This was due to burst splitting events that caused the processor to over-count drops [22–25], which is discussed further below. The processor settings used when collecting the data presented in this paper were: mixer frequency = 40 MHz, sample frequency = 10 MHz, low pass filter = 1.25 MHz. Hardware coincidence, which requires that drops be detected on both PDI channels simultaneously, was used as an additional validation criteria for all measurements. An intensity validation scheme was utilized to account for trajectory-dependent scattering errors [26–33]; however, the occurrence of such errors was found to be minimal. The intensity validation scheme

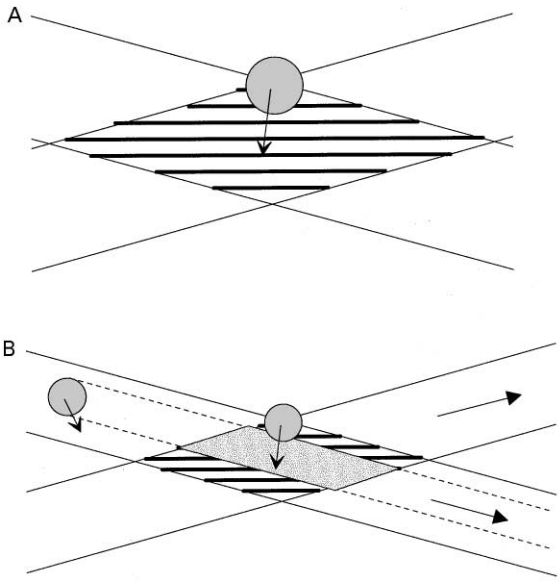

Fig. 3. Schematic of (A) a droplet crossing through the sample volume and (B) the phenomenon leading to burst splitting events in PDI measurements.

also enables the identification and rejection of large drops that are erroneously sized as small drops due to exceeding the optical range of the PDI system [15]. Additional details of the experimental apparatus and procedure are available in Ref. [15].

3. Results and discussion

3.1. Doppler burst splitting

The large coverage area of the sprays investigated here requires that the optical components (transmitting and receiving optics) of the PDI be located within the spray, as shown in Fig. 1. As a result, the spray outside of the measurement volume can have an impact upon the measurements. In particular, when characterizing the water drops in these sprays using PDI, the attenuation of the laser beams due to droplets passing through the laser beams must be considered. As drops pass through the laser beams, significant intensity fluctuations may result, and the beam coherence adversely affected. This is depicted in Fig. 3B. It was discovered that the impact of the laser beam attenuation on the beam coherence in the sample volume was significant, and led to over-counting of drops, as discussed by Widmann et al. [24,25]. In short, Doppler burst signals are degraded and erroneously interpreted by the PDI processor as multiple bursts. This is shown in Fig. 4, where oscilloscope traces of the gate and Doppler signals are presented. Fig. 4A shows a single Doppler

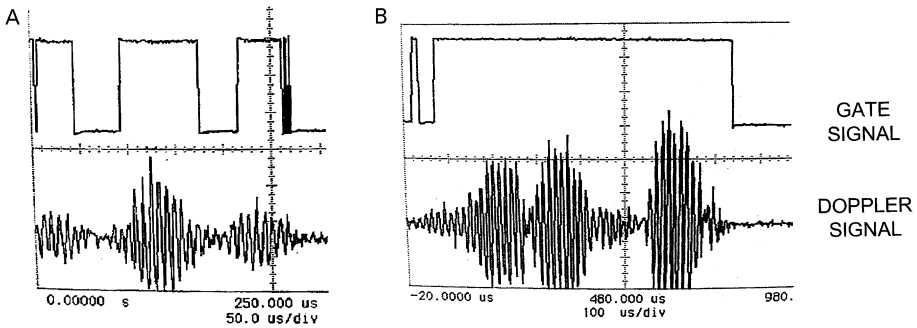

Fig. 4. Oscilloscope traces of the gate signal and Doppler signal during PDI measurements in sprinkler sprays. Over-counting of the drops due to burst splitting events are shown in (A), and a case in which a single drop was correctly counted is shown in (B).

burst that has been split into three bursts due to drops passing through and attenuating the laser beams. The split Doppler burst shown in Fig. 4A results in over-counting by the PDI processor.

Fig. 5 presents PDI volume flux measurements obtained in the spray produced by sprinkler *D* compared to pan test measurements obtained at the same location with a stop watch and graduated cylinder. Note that although the measurement area for the pan tests ($31.4\,\mathrm{cm}^2 \pm 1.0\,\mathrm{cm}^2$) is considerably larger than that of the PDI measurements (of order $0.01\,\mathrm{cm}^2$), it is orders of magnitude smaller than the area of the spray (approximately $10\,\mathrm{m}^2$). The characteristics of the spray do not vary significantly over the dimensions of the pan test measurement area, and therefore the fluxes determined from the pan tests can be compared directly with those obtained from the PDI measurements. The filled symbols in Fig. 5 correspond to the PDI manufacturer's recommended sampling parameters. It is clear that using these sampling parameters results in the PDI measuring the volume flux significantly too high. The open symbols in Fig. 5 correspond to the PDI operating conditions used for the measurements presented here. The agreement between the PDI volume flux measurement and the pan test measurement is much better in this case. The vertical error bars in Fig. 5 represent only the Type A uncertainties ($2\,s$). The horizontal error bars represent the 6.6% combined standard uncertainty, $2U_c$, of the pan test measurements. This uncertainty includes both Type A and Type B uncertainties, and therefore accounts for experimental errors in addition to the variance of the replicated measurements [16,17].

The large error in the volume flux measurements when operating the PDI with the recommended operating conditions is due to the burst splitting events depicted in Fig. 3B. The split Doppler bursts result in the processor both over-counting drops and also incorrectly calculating the probe area. Both of these effects contribute to the large error in the flux measurements. Reducing the sample frequency of the PDI from 40 to 10 MHz increases the likelihood that the processor will sample through the brief periods in which the coherence of the laser beams is degraded without detecting the departure of the drop from the probe volume. This is shown in Fig. 4B,

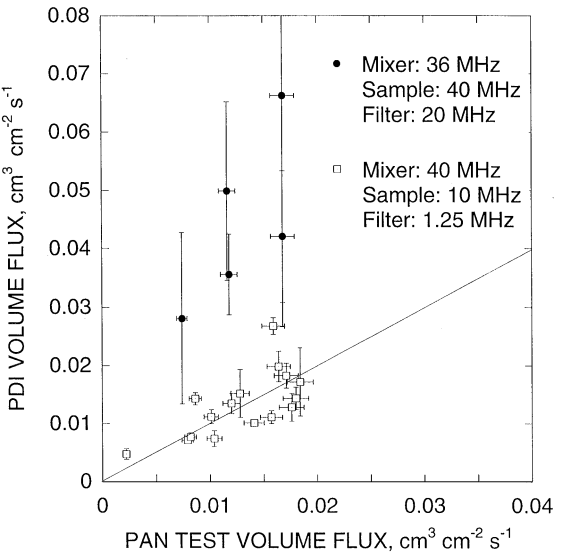

Fig. 5. Comparison of the PDI volume flux measurements and pan test volume flux measurements for residential fire sprinkler *D*. The PDI operating conditions are discussed in the text.

where the gate signal and Doppler signal corresponding to measurements obtained with a sample rate of 10 MHz are presented. In this case, the PDI processor correctly interprets the Doppler signal as a single drop despite the degraded beam coherence. Reducing the sample rate effectively improves the signal-to-noise ratio (SNR) because the discrete sampling detects less of the high frequency noise. Because the SNR is used to detect the arrival and departure of drops from the probe volume, increasing the SNR reduces the likelihood that the processor will erroneously interpret split bursts as multiple drops. The reader is referred to Refs. [24,25] for a complete discussion of burst splitting events in phase Doppler interferometry measurements.

3.2. Spray characterization

Fig. 6 presents representative size distributions collected at two locations in the spray produced by the sprinkler *D*. In each case, three size distributions, corresponding to replicated measurements at the same location, are shown to demonstrate the variability in the runs. The size distributions presented in Figs. 6A and B correspond to data collected close to ($r < 0.5$ m) and far from ($r > 1.5$ m) the sprinkler axis, respectively. In general, data collected close to the sprinkler axis resulted in estimated size distributions that are represented reasonably well by a log-normal model. Data obtained farther from the sprinkler, which are more heavily weighted by larger drops, resulted in size distributions more accurately modeled by Rosin–Rammler size distributions [34]. You [10] reported that measured size

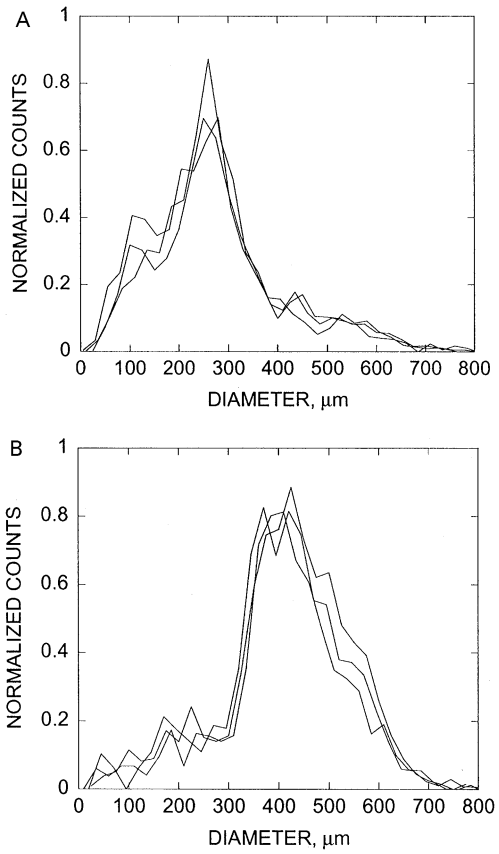

Fig. 6. Representative size distributions obtained with the PDI system at locations (A) near and (B) far from the axis of residential fire sprinkler *D*.

distributions were best represented by a modified size distribution model in which the smaller drops were represented by a log-normal distribution and the larger drops were represented by a Rosin–Rammler model. Current efforts in our laboratory include representing size distributions at all locations in the spray as a weighted mixture of log-normal and Rosin–Rammler distributions. Such a size distribution model could easily be incorporated into computational models intended to predict the interaction of fires and the water sprays produced by the experimentally characterized sprinklers.

The upper limit of the drop size for the measurements presented is 950 μm, which is determined by the optical system of the PDI. The size distributions presented in Fig. 6 show that the number of drops exceeding the upper size limit is small. Furthermore, because the volume flux is heavily influenced by the large drops, the good agreement between the pan test measurements and the PDI volume flux measurements indicate that very few large drops are missed. The fact that large

drops passing through the probe volume would result in signal saturations, and that very few saturations were observed during the measurements, provides further evidence that the PDI size range used was appropriate.

The phase Doppler interferometry system used here simultaneously measures the size and two components (axial and radial) of velocity of the drops that pass through the probe volume. By measuring the characteristics of a large number of drops, size and velocity distributions can be estimated. Furthermore, the volume flux of the liquid phase through the probe volume can be determined provided that the cross-sectional area of the probe volume is known or can be estimated. Current generations of PDI systems calculate the probe area in situ from the transit time and velocity of the measured droplets [15,21,26,35].

To summarize the large volume of experimental data corresponding to spray characterization in a concise manner, characteristic sizes are frequently calculated from experimental size distributions. In this paper, three characteristic sizes are presented as a function of the radial coordinate in the spray. The characteristic sizes presented here are the arithmetic mean diameter (D_{10}), the volume mean diameter (D_{30}), and the Sauter mean diameter (D_{32}). These are defined as [36]

$$D_{10} = \frac{\sum_i n_i d_i}{\sum_i n_i}, \tag{1}$$

$$D_{30} = \left(\frac{\sum_i n_i d_i^3}{\sum_i n_i} \right)^{1/3} \tag{2}$$

and

$$D_{32} = \frac{\sum_i n_i d_i^3}{\sum_i n_i d_i^2}, \tag{3}$$

where n_i and d_i are the number of counts in the ith size class and the drop diameter corresponding to the ith size class, respectively. Note that the number of counts in each size class, n_i, must be corrected for the size dependence of the probe volume [35]. Eqs. (1)–(3) correspond to the conventional engineering definitions, as opposed to the statistical definitions [37].

Fig. 7 summarizes the PDI measurements obtained in sprinkler A as a function of the radial and angular coordinates. The operating pressures corresponding to the measurements are presented in Table 1. The angular coordinate is defined such that $\theta = 0^\circ$ corresponds to the location of one of the yoke arms (see Fig. 2). The angular variation presented in Fig. 7 is typical of the sprinklers characterized in this study. It is apparent that the mean axial velocity, mean radial velocity, and the volume mean diameter are relatively constant with angular position. Only the volume flux shows significant variation as a function of the angular coordinate. Factors contributing to the variation in the volume flux measurements include the stochastic nature of the spray, uncertainties in the volume flux measurements, and asymmetry in the sprinkler spray. The variation in the volume flux measurements for sprinkler A, shown in Fig. 7A, was greater than the variation in the volume flux measurements for the sprays produced by the other three sprinklers. This is related to the lower

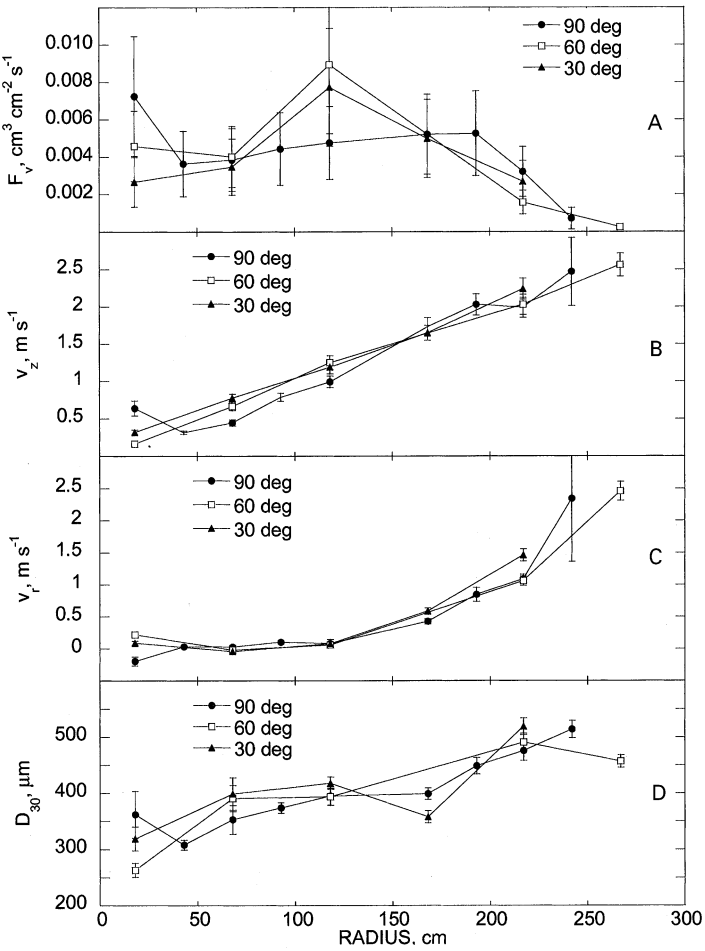

Fig. 7. Angular variation of the (A) volume flux, (B) axial velocity, (C) radial velocity, and (D) volume mean diameter for sprinkler *A*.

pressure at which this sprinkler was operated. It was observed that, in general, angular variations in the volume flux measurements decreased with increasing water pressure.

The characteristic mean sizes for the four sprinklers are presented in Fig. 8. The profiles represent data averaged over various angular coordinates, θ, in a horizontal plane $1.12\,\mathrm{m} \pm 0.01\,\mathrm{m}$ below the sprinkler head. For example, the spray data presented in Fig. 8D (sprinkler *D*) correspond to 370 samples collected at 120 locations in the spray. A sample consisted of 2000 drop attempts (instances when a drop passes through the probe volume). The actual number of drops measured was less than this because not all signals were validated. Collecting larger sample sizes was impractical due to the low data rates associated with this low number density

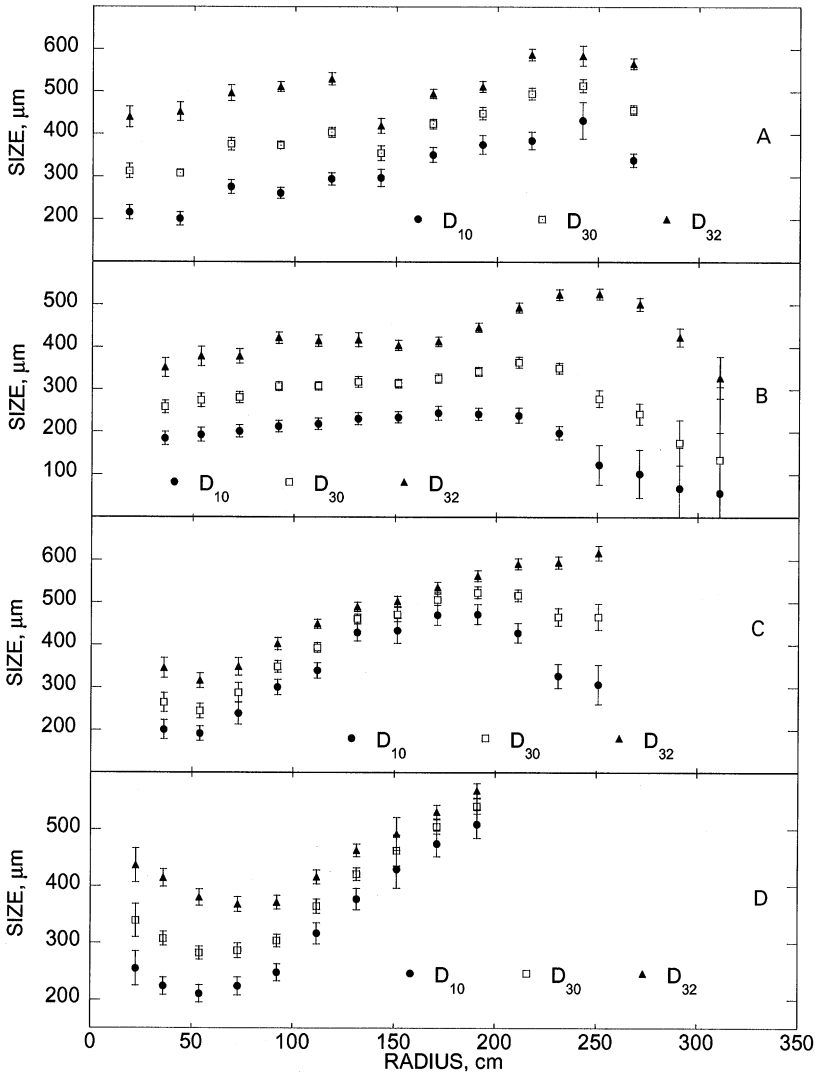

Fig. 8. Characteristic sizes of the water drops measured in the sprays produced by (A) sprinkler *A*, (B) sprinkler *B*, (C) sprinkler *C*, and (D) sprinkler *D*.

spray. Data rates typically varied from 0.1 to 10 Hz, depending upon the measurement location.

The data in Fig. 8 indicate that, in general, the characteristic sizes increase with radial coordinate. For example, in the sprays generated by the two sprinklers (sprinklers *C* and *D*) with *K*-factors [38] of $1.35 \times 10^{-4}\,\mathrm{m^3\,s^{-1}\,kPa^{-0.5}}$ and identical flow rates, the arithmetic mean diameter, D_{10}, varied from approximately 200 μm where the size distributions were heavily weighted by the smaller drops to 450 or

500 μm in the outer region of the spray (see Figs. 8C and D). For large values of the radial coordinate, r, the size distributions are dominated by larger drops because the smaller drops have insufficient initial momentum to reach the outer spray region. The smaller drops that are detected at the outer region of the spray are likely carried by the bulk flow of the ambient air. The momentum exchange between the spray and air results in recirculation zones directly beneath the sprinkler head and near the outer regions of the spray. This is shown pictorially in Fig. 9. As will be shown below, the volume flux corresponding to the radial coordinates where the mean sizes are decreasing with increasing r is low, and represents a small fraction of the total flow of water through the sprinkler. The mean size and velocity in these locations is decreasing due to the many small drops that are entrained into the spray by the surrounding gas.

In contrast to sprinklers C and D, the arithmetic mean diameter measured in sprinkler B shows significantly less dependence upon the radial coordinate. The value of D_{10} presented in Fig. 8B remains approximately 200 μm over the entire radial profile, but shows a slight increase with r. Sprinkler A produces a spray with mean droplets sizes (D_{10}) that increase with r and vary between approximately 200 and 400 μm, as shown in Fig. 8A.

The mean axial and radial velocities measured in the four sprays are presented in Fig. 10. Consistent with the mean sizes presented in Fig. 8, the data correspond to measurements that have been averaged over numerous angular coordinates. Three of the sprinklers produce sprays with mean axial velocities that peak around $2.5\,\mathrm{m\,s^{-1}}$, as shown in Figs. 10A, C, and D. The mean axial velocity of the drops produced by sprinkler B, shown in Fig. 10B, only reaches a maximum value of roughly $1.5\,\mathrm{m\,s^{-1}}$. The lower value of the axial velocity can be attributed to the smaller size of the drops produced by this sprinkler (see Fig. 8B). The small drops leave the sprinkler head with less momentum than large drops, and decelerate more rapidly. Fig. 11 presents the axial velocity with respect to droplet size from one of the data sets collected in sprinkler B. Note that most of the drops have velocities higher than the corresponding terminal velocities, which indicates that the drops left the sprinkler with greater momentum and have not yet decelerated to the terminal velocity at the measurement plane. The bulk air motion shown in Fig. 9 may also be adding to the drop velocity. Although the mean velocity corresponding to this sprinkler does not exceed $1.6\,\mathrm{m\,s^{-1}}$ at the measurement plane, many of the drops do have higher

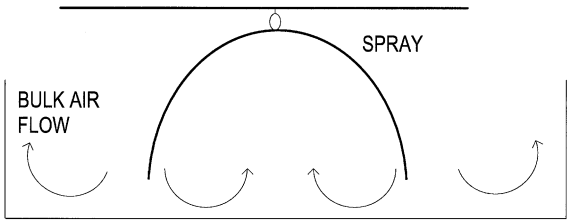

Fig. 9. Recirculation zones in the experimental facility due to momentum exchange between the spray and the ambient air.

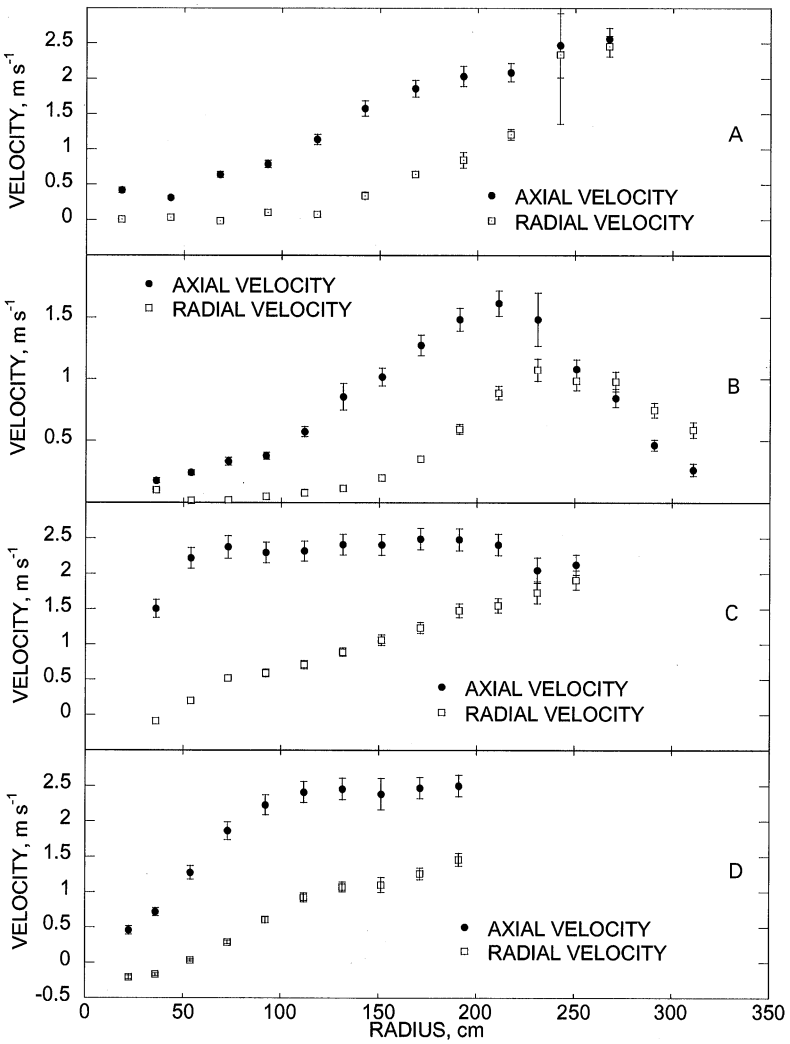

Fig. 10. Axial and radial velocities of the water drops measured in the sprays produced by (A) sprinkler *A*, (B) sprinkler *B*, (C) sprinkler *C*, and (D) sprinkler *D*.

velocities. The large number of small drops, with corresponding low velocities, heavily influence the mean value and result in the mean velocities presented in Fig. 10B. The stratification apparent in Fig. 11 is due to the way that the velocity data are binned by the PDI software and is discussed in Ref. [15] along with the measurement uncertainties.

The mean radial component of the drop velocity is approximately zero near the sprinkler axis, and increases with radial coordinate, as would be expected. It is interesting to note that the spray produced by sprinkler *D* contains drops with

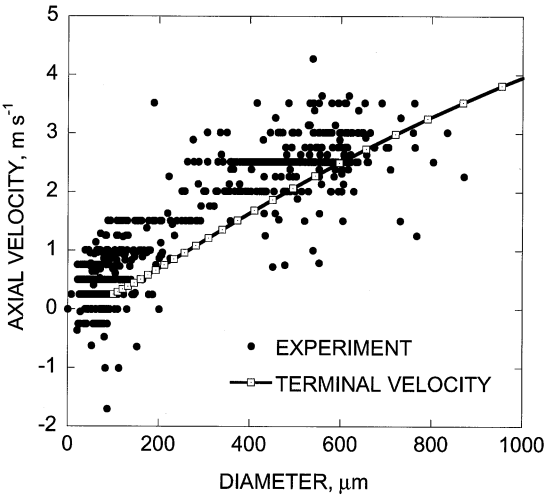

Fig. 11. Axial velocity with respect to drop size for one location in the spray produced by sprinkler *B*.

negative mean radial velocities close to the sprinkler axis (see Fig. 10D). This is due to the recirculation zone depicted in Fig. 9.

The radial profiles of the volume flux measurements in the four sprinklers are presented in Fig. 12. The data indicate that the spray pattern is significantly different for each sprinkler. For example, the volume flux measurements for sprinkler *D* reveal that most of the water spray at this horizontal plane (1.12 m below the sprinkler) flows through an annular ring approximately 0.5 m wide and centered at $r \approx 1.2$ m. Sprinkler *B* also delivers most of the water in an annular ring. In this case, the water is delivered through a ring approximately 1 m wide and centered at $r \approx 1.9$ m. The delivery pattern of sprinkler *C* peaks very close to the sprinkler axis, and decreases slowly with radial coordinate (see Fig. 11C). There is more variability in the radial profile of the volume flux measurements for sprinkler *A*, which contains peaks at $r \approx 1.2$ and 1.9 m. Note that this sprinkler was operated at the lowest water pressure. As with the angular variation shown in Fig. 7A, the radial variation in the volume flux measurements were found to decrease with increasing water pressure.

The angular variation in the volume flux measurements was greater than the size or velocity measurements, which was shown in Fig. 7. This may be attributed to the presence of the yoke arms that hold the deflector plate in place, the grooves on the deflector plate, the stochastic nature of the spray process, or the inherent uncertainty in PDI volume flux measurements. Although the volume flux measurements display greater variation with the angular coordinate than the size and velocity measurements, there is no obvious dependency on θ. This may be due to the randomness of the spray or insufficient measurement resolution. PDI is capable of measurements with very fine resolution; however, the large coverage area of the sprinkler spray makes such measurements impractical. The need to collect large quantities of data to characterize a single spray is the primary disadvantage of using PDI in very large

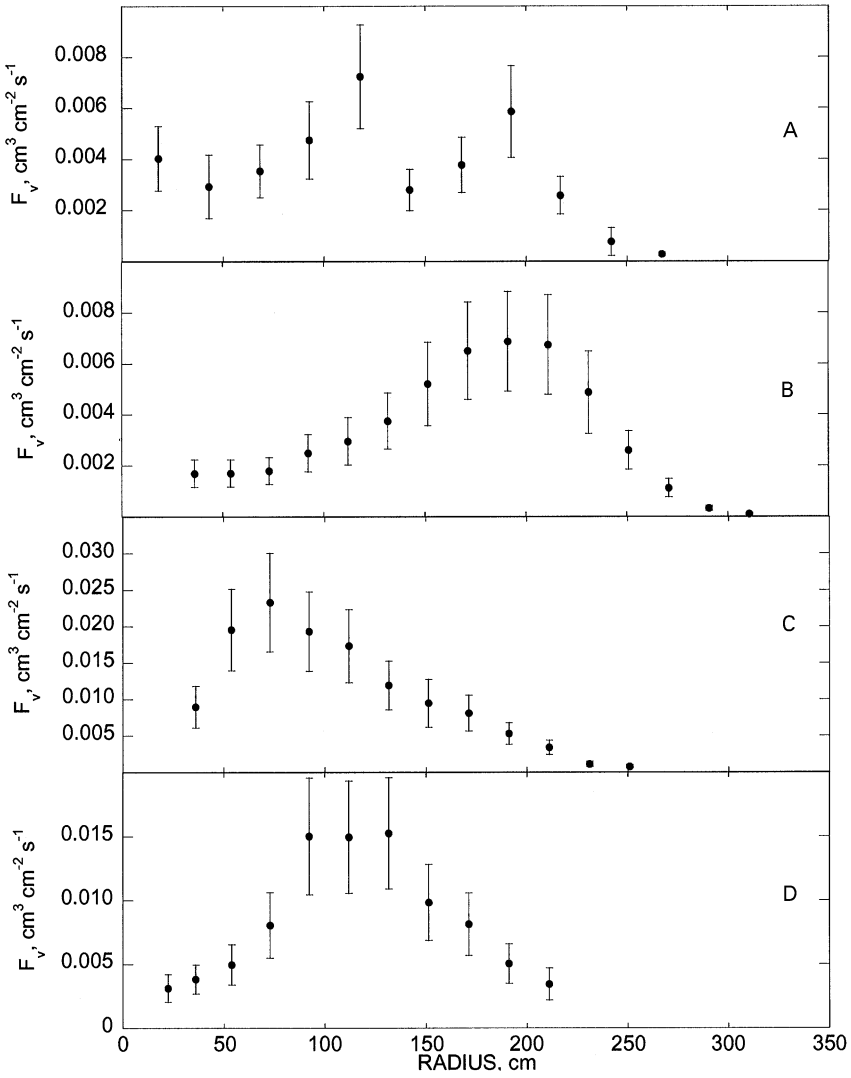

Fig. 12. Volume flux of water drops measured in the sprays produced by (A) sprinkler *A*, (B) sprinkler *B*, (C) sprinkler *C*, and (D) sprinkler *D*.

sprays like the one investigated here. Regardless of the cause, averaging over the angular coordinate, and including the angular variations in the Type A uncertainties as was done in Fig. 12, results in useful volume flux profiles with reasonable measurement uncertainties, appropriate for use in fire dynamics models. Volume flux profiles measured close to the sprinkler can be used as input conditions for the simulations, while measurements further downstream can be used to validate the predictions of the model.

The volume flux profile shown in Fig. 12 can be integrated over the radial coordinate to obtain a flow rate through the measurement plane, which can be compared with the flow rate of water through the sprinkler. The volumetric flow rate, V, through the sprinkler can be determined from the K-factor and the pressure at the sprinkler head using the relation

$$V = KP^{0.5}, \tag{4}$$

where K is the numerical K-factor in the appropriate units and P is the water pressure (gauge) at the sprinkler head. The K-factors reported by the manufacturers, and the operating pressures, are summarized in Table 1 for the sprinklers used here. The flow rates determined from Eq. (4) and integrating the volume flux measurements across the measurement plane are presented in Table 2. The integrated flow rates agree with the value calculated from the sprinkler K-factor to within 5%, 7%, 8%, and 8%, for sprinklers A, B, C, and D, respectively. Note that the uncertainty in the flow rate determined from the PDI measurements are approximately 10% (see Table 2), and therefore the PDI measurements agree with the flow rates determined from the K-factors and operating pressures to within the measurement uncertainty. The good agreement indicates that the volume flux profiles presented in Fig. 12 are consistent with the total flow of water through the sprinkler. Furthermore, the good agreement ensures that if there are drops in the spray that are too large to be sized by the instrument, they constitute a small fraction of the total mass of the spray, as discussed above.

Using the data presented in Figs. 8 and 12, a flux-averaged mean volume diameter, $\overline{D_{30}}$, for the entire spray can be calculated from

$$\overline{D_{30}} = \frac{\int_0^\infty D_{30}(r)F_v(r)r\,\mathrm{d}r}{\int_0^\infty F_v(r)r\,\mathrm{d}r}, \tag{5}$$

where $F_v(r)$ is the volumetric flux at r. The calculations are illustrated by the two plots in Fig. 13, which correspond to sprinkler B. Here, the integrands of the integrals in the numerator and denominator of Eq. (5) are presented as a function of the radial coordinate, r. Note that the volume flux is assumed to be negligible at $r = 0$ and 4 m. The values of $\overline{D_{30}}$ calculated from Eq. (5) are summarized in Table 2 for the sprays investigated here. This is a useful parameter for concisely quantifying the drop size of a sprinkler spray. Combined with the volume flux data, it can also be

Table 2
The calculated flow rate through the sprinkler based upon the sprinkler K-factors and PDI measurements, and the mean volume diameter based upon Eq. (5)

Sprinkler	K-factor flow rate ($m^3\,s^{-1} \times 10^3$)	PDI flow rate ($m^3\,s^{-1} \times 10^3$)	$\overline{D_{30}}$ (μm)
A	0.733 ± 0.05	0.792 ± 0.08	427 ± 17
B	0.978 ± 0.05	1.03 ± 0.11	356 ± 15
C	1.54 ± 0.05	1.67 ± 0.18	409 ± 17
D	1.54 ± 0.05	1.43 ± 0.15	422 ± 17

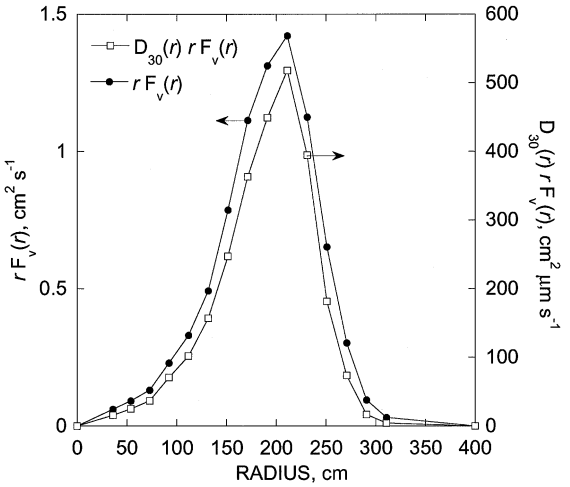

Fig. 13. Data for sprinkler *B* showing the calculation of the flow rate through the sprinkler and the mean volume diameter as defined in Eq. (5).

useful for preliminary modeling efforts to explore the interaction of the sprinkler spray with a fire. For example, the adequacy of submodels for drop transport and evaporation can be investigated for a drop size corresponding to the actual spray without introducing the complications associated with polydisperse spray systems.

3.3. *Effect of water pressure*

You [10] reported that at room temperature, the characteristic drop size produced by a specific sprinkler head is proportional to $P^{-1/3}$. Such a relation is of significant practical value because not all applications will have the same water pressure available for the fire sprinkler system, and it is impractical to make droplet measurements over the entire range of possible activation pressures. Furthermore, in a fire scenario in which multiple sprinklers are activated, the water pressure typically decreases as additional sprinklers are activated. Although very useful for drop size predictions, this relation is based upon theoretical arguments, and has not been experimentally verified. You [10] presented some limited laser-light shadowing measurements, but unfortunately only two pressures were investigated (206 and 393 kPa), making it difficult to draw conclusions about the applicability of this size/pressure relation.

To explore the effect of the water pressure on the mean drop size, measurements were obtained in the spray produced by sprinkler *B* under various operating pressures, and Eq. (5) was applied to determine the flux-averaged volume diameter for each case. The water pressure to the sprinkler head was varied from 69 kPa (10 psig) to 200 kPa (29 psig). Fig. 14 presents the flux-averaged volume diameter, $\overline{D_{30}}$, with respect to the operating pressure to the $-1/3$ power, $P^{-1/3}$. The data presented in Fig. 14 follow a linear trend, consistent with the relation presented by

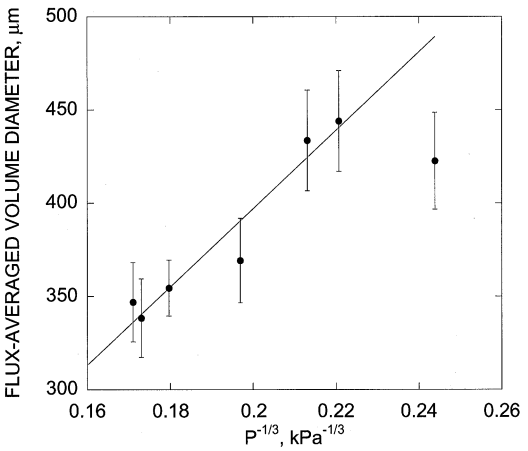

Fig. 14. Flux-averaged volume diameter, $\overline{D_{30}}$, defined in Eq. (5), as a function of the water pressure.

You [10], except for one data point. The solid line in Fig. 14 corresponds to a least-squares fit to the data excluding the outlier, and the correlation coefficient is $R = 0.9679$. The outlier in Fig. 14 corresponds to the lowest operating pressure investigated, $P = 69$ kPa, and may represent a pressure at which the correlation is no longer valid. Note that the $P^{-1/3}$ dependence predicts an infinite drop size as the pressure goes to zero. Thus, it is evident that the relation will break down at low operating pressure. The data presented in Fig. 14 indicate that the relation is valid to $P = 93$ kPa, but additional work is required to determine the pressure dependence of the mean drop size at lower operating pressures.

4. Conclusion

Four residential pendant sprinklers have been experimentally characterized using Phase Doppler interferometry. The results indicate that PDI is a useful method of providing input and validation data for fire dynamics simulations by measuring the size, velocity, and volume flux of drops produced by residential fire sprinklers. The data indicate that, in general, the characteristic sizes increase with radial coordinate. For large values of the radial coordinate, r, the size distributions are dominated by larger drops because the smaller drops have insufficient initial momentum to reach the outer spray region. The smaller drops that are detected at the outer region of the spray are likely carried by the bulk flow of the ambient air.

Three of the sprinklers produce sprays with mean axial velocities that peak around $2.5\,\mathrm{m\,s^{-1}}$, whereas the mean axial velocity of the drops produced by sprinkler B only reaches a maximum value of roughly $1.5\,\mathrm{m\,s^{-1}}$. The lower value of the axial velocity can be attributed to the smaller size of the drops produced by this sprinkler under these operating conditions. The small drops leave the sprinkler head with less momentum than large drops, and decelerate more rapidly.

The effect of the sprinkler operating pressure on the mean drop size was investigated. The theoretical relation between the operating pressure and the mean drop size presented by You [10] was experimentally tested and found to be valid over the range $93\,\text{kPa} \leqslant P \leqslant 200\,\text{kPa}$ for one type of residential sprinkler. Mean drop size measurements obtained at 69 kPa did not follow the expected behavior, suggesting that the correlation is not valid at such low pressures.

The primary disadvantage of using PDI in fire sprinkler sprays is that it is a single-point diagnostic method, and therefore accurately mapping an entire spray can be a tedious and time-consuming process.

Acknowledgements

The author would like to acknowledge Stefan Leigh for his assistance in determining the uncertainties in the reported measurements, and Cary Presser for the use of the PDI system. Also, the contributions of Jacob Goodman and Daniel Landau were invaluable in the data collection stage of this work.

References

[1] Yao C, Kalelkar AS. Effect of drop size on sprinkler performance. 74th annual meeting of the national fire protection association, Toronto, 1970. p. 254–68.
[2] Grant G, Brenton J, Drysdale D. Fire suppression by water sprays. Prog Energy Combust Sci. 2000;26:79–130.
[3] Baum HR, McGrattan KB, Rehm RG. Three dimensional simulations of fire plume dynamics. J Heat Transfer Soc Japan 1997;35:45–52.
[4] McGrattan KB, Baum HR, Rehm RG. Large eddy simulations of smoke movement. Fire Safety J 1998;30:161–78.
[5] Lawson JR, Walton WD, Evans DD. Measurement of droplet size in sprinkler sprays. National Bureau of Standards, U.S. Department of Commerce, NBSIR 88-3715, Gaithersburg, MD, February 1988.
[6] Nolan PF. Feasibility study of using laser high speed cine systems for the characterization of droplets from sprinkler sprays. The Swedish Fire Research Board, Stockholm, Sweden, 1989.
[7] Jackman LA, Nolan PF, Morgan HP. Characterization of water drops from sprinkler sprays. Fire Suppression Research — First International Conference, Stockholm, Sweden, 1992. p. 159–84.
[8] Chow WK, Shek LC. Physical properties of a sprinkler water spray. Fire Mater 1993;17:279–92.
[9] You HZ. Sprinkler drop-size measurement, Part II: an investigation of the spray patterns of selected commercial sprinklers with the FMRC PMS droplet measuring system. Technical Report 0G1e7.RA 070(A), Norwood, MA, May 1983.
[10] You HZ. Investigation of spray patterns of selected sprinklers with the FMRC drop size measuring system. Fire Safety Science — Proceedings of the First International Symposium, Gaithersburg, MD, October 1985. p. 1165–76.
[11] Chan TS. Measurements of water density and drop size distributions of selected ESFR sprinklers. J Fire Prot Engr 1994;6:79–87.
[12] Putorti AD, Belsinger TD, Twilley WH. Determination of water spray drop size and speed from a standard orifice, Pendent Spray Sprinkler. Report of Test. National Institute of Standards and Technology, Gaithersburg, MD, May 1999.

[13] Sheppard DT, Gandhi PD, Lueptow RM. Predicting sprinkler water distribution using particle image velocimetry. Research and Practice: Bridging the Gap. National Fire Protection Research Foundation, Orlando, FL, February 1999.
[14] Gandhi PD, Steppan D. Using PDPA in evaluation of sprinklers. Proceedings Fire Suppression and Detection Research Application Symposium. Research and Practice: Bridging the Gap. National Fire Protection Research Foundation, Orlando, FL, February 1999. p. 65–78.
[15] Widmann JF. Characterization of a residential fire sprinkler using Phase Doppler Interferometry. Atomization Sprays, 2000, submitted.
[16] Taylor BN, Kuyatt CE. Guidelines for evaluating and expressing the uncertainty of NIST measurement results. NIST Technical Note 1297, National Institute of Standards and Technology, Gaithersburg, MD, September 1994.
[17] American National Standard for Expressing Uncertainty—U.S. Guide to the Expression of Uncertainty in Measurement. ANSI/NCSL Report Z540-2-1997, National Conference of Standards Laboratories, Boulder, CO, October 1997.
[18] Durst F, Zare M. Laser Doppler measurements in two-phase flows. Proceedings of the LDA Symposium, Copenhagen, 1975. p. 403–29.
[19] Bachalo WD, Houser MJ. Development of the phase/doppler spray analyzer for liquid droplet size and velocity characterization. AIAA/SAE/ASME 20th Joint Propulsion Conference, 1984.
[20] Bachalo WD, Houser MI. Phase/Doppler spray analyzer for simultaneous measurements of droplet size and velocity distributions. Opt Eng 1984;1:583–90.
[21] Bachalo WD. Experimental methods in multiphase flows. Int J Multiphase Flow 1994;20:261–95.
[22] Van Den Moortel T, Santini R, Tadrist L, Pantaloni J. Experimental study of the particle flow in a circulating fluidized bed using a phase Doppler particle analyzer: a new post-processing data algorithm. Int J Multiphase Flow 1997;23:1189–209.
[23] Lazaro BJ. Evaluation of phase Doppler particle sizing in the measurement of optically thick, high number density sprays. United Technologies Research Center, East Hartford, Connecticut, Report UTRC 91-11, 1991.
[24] Widmann JF, Presser C, Leigh SD. Effect of burst splitting events on phase Doppler interferometry measurements. 30th AIAA Aerospace Sciences Meeting, Paper 2001-1130, Reno, NV USA, January 8–11, 2001.
[25] Widmann JF, Presser C, Leigh SD. Identifying burst splitting events in phase Doppler interferometry measurements. Atomization Sprays, 2000, submitted.
[26] Sankar SV, Bachalo WD. Response characteristics of the phase-Doppler particle analyzer for sizing spherical particles larger than the wavelength. Appl Opt 1991;30:1487–96.
[27] Sankar SV, Inenaga AS, Bachalo WD. Trajectory dependent scattering in phase Doppler interferometry: minimizing and eliminating sizing errors. In: Adrian RJ, Durão DFG, Durst F, Heitor MV, Maeda M, Whitelaw JH, editors. Laser Techniques and Applications in Fluid Mechanics. Berlin: Springer-Verlag, 1992. p. 75–89.
[28] Gréhan G, Gouesbet G, Naqwi A, Durst F. Trajectory ambiguities in phase Doppler systems: study of a near forward and a near backward geometry. Part Part Syst Charact. 1994;11:133–44.
[29] Hardalupas Y, Taylor AMKP. Phase validation criteria of size measurements for the phase Doppler technique. Expts Fluids 1994;17:253–8.
[30] Schaub SA, Alexander DR, Barton JP. Theoretical analysis of the effects of particle trajectory and structural resonances on the performance of a phase Doppler particle analyzer. Appl Opt 1994;33:473–83.
[31] Sankar SV, Bachalo WD, Robart DA. An adaptive intensity validation technique for minimizing trajectory dependent scattering errors in phase Doppler interferometry. Fourth International Congress on Optical Particle Sizing, Nuremberg, Germany, March 21-23, 1995.
[32] Hardalupas Y, Liu CH. Implications of the Gaussian intensity distribution of laser beams on the performance of the phase Doppler technique. Progr Energy Combustion Sci 1997;23:41–63.
[33] Qui H, Hsu CT. Method of phase-Doppler anemometry free from the measurement volume effect. Appl Opt 1999;38:2737–42.

[34] Rosin P, Rammler E. The laws governing the fineness of powdered coal. The Institute of Fuel, October, 1933, pp. 29–36.
[35] Widmann JF, Presser C, Leigh SD. Improving phase Doppler volume flux measurements in low data rate applications. Meas Sci Technol, 2000, submitted.
[36] Mugele RA, Evans HD. Droplet size distribution in sprays. Ind Eng Chem 1951;43:1317–24.
[37] Sowa WA. Interpreting mean drop diameters using distribution moments. Atomization Sprays 1992;2:1–15.
[38] Fleming RP. Automatic sprinkler system calculations. In: The SFPE handbook of fire protection engineering, 2nd ed. National Fire Protection Association, Quincy, MA, June 1995.